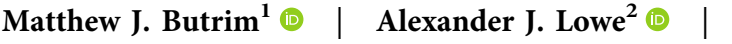
#### RESEARCH ARTICLE



Check for updates

# Leaf mass per area: An investigation into the application of the ubiquitous functional trait from a paleobotanical perspective



Ellen D. Currano<sup>1</sup>

<sup>2</sup>Department of Biology, University of Washington, Seattle, Washington 98195, USA

#### Correspondence

Matthew J. Butrim, Department of Geology and Geophysics, Program in Ecology, University of Wyoming, Laramie, Wyoming 82071, USA. Email: mbutrim@uwyo.edu

#### Abstract

Premise: Leaf mass per area (LMA) is a widely used functional trait in both neobotanical and paleobotanical research that provides a window into how plants interact with their environment. Paleobotanists have used site-level measures of LMA as a proxy for climate, biome, deciduousness, and community-scale plant strategy, yet many of these relationships have not been grounded in modern data. In this study, we evaluated LMA from the paleobotanical perspective, seeking to add modern context to paleobotanical interpretations and discover what a combined modern and fossil data set can tell us about how LMA can be best applied toward interpreting plant communities.

Methods: We built a modern data set by pulling plant trait data from the TRY database, and a fossil data set by compiling data from studies that have used the petiole-width proxy for LMA. We then investigated the relationships of species-mean, site-mean, and site-distribution LMA with different climatic, phylogenetic, and physiognomic variables.

Results: We found that LMA distributions are correlated with climate, site taxonomic composition, and deciduousness. However, the relative contributions of these factors are not distinctive, and ultimately, LMA distributions cannot accurately reconstruct the biome or climate of an individual site.

Conclusions: The correlations that make up the leaf economics spectrum are stronger than the correlations between LMA and climate, phylogeny, morphospace, or depositional environment. Fossil LMA should be understood as the culmination of the influences of these variables rather than as a predictor.

### KEYWORDS

community ecology, functional trait, leaf economics spectrum, leaf mass per area, LMA, paleobotany, paleoclimate, proxy, specific leaf area, TRY database

Functional traits are often heralded as the future of paleobiology (Eronen et al., 2010; Barnosky et al., 2017; Vermillion et al., 2018). Trait-based ecology can be ataxonomic to an extent, and thus has the potential to reveal some of the fundamental patterns and correlations that persist from ancient to present-day ecosystems. To uncover these patterns, there has been a rush toward discovering new ways of reconstructing functional traits from the fossil record. Paleobotany is no stranger to this trend, and one of its most rapidly adopted methods has been the petiole-width proxy for leaf dry mass per area (LMA; Royer et al., 2007). LMA is a powerful plant functional trait that, in quantifying the combined thickness and density of a leaf, represents plant investment per

area of light intercepting surface (Gutschick and Wiegel, 1988; Poorter et al., 2009). Additionally, LMA is a foundational component of the leaf economics spectrum, a suite of tightly covarying traits that also includes leaf life span, photosynthetic rate, respiration rate, and nitrogen and phosphorus investment (Wright et al., 2004). LMA by itself, then, can indicate whether a leaf (Wright et al., 2004), and to some extent an entire plant (Reich, 2014; but see Díaz et al., 2016), follows a fast (low-LMA) or slow (high-LMA) return-on-investment strategy. For fossil flora, this property is invaluable, allowing a commonly preserved, yet highly plastic, organ of the plant to become a reliable representative of how the whole plant may have interacted with its environment.

<sup>&</sup>lt;sup>1</sup>Department of Geology and Geophysics, Program in Ecology, University of Wyoming, Laramie, Wyoming 82071, USA

As a result, the petiole-width proxy for LMA has become a standard component of the paleobotanical toolbox. The method only requires measurements of the area of the fossil leaf and the width of the petiole at the base of the leaf lamina to approximate the direct measurements of fresh leaf area and dry leaf mass made by neobotanists (Royer et al., 2007). As a result, fossil reconstructions of LMA are broadly accessible, and LMA can typically be reconstructed for a sizable proportion of the morphospecies (form taxa differentiated with leaf architecture; Ellis et al., 2009) at a given fossil locality. This allows paleobotanists to go beyond species-mean LMA values, which only reflect the average LMA of one morphospecies, and instead attempt to reconstruct ecological characteristics of an entire locality. By including all of a site's measured morphospecies, paleobotanists can reconstruct site-mean LMA, an average of the species-mean LMA values, and LMA distribution, a probability distribution function extrapolated from the spread of species-mean LMA values (e.g., Royer et al., 2007; Roth-Nebelsick et al., 2017; Butrim and Royer, 2020).

Site-mean LMA reconstructions tend to be used as counterparts to species-mean LMA, with interpretations simply scaled up to represent an entire locality. For example, site-mean LMA can provide the basis for hypotheses about the economic tendencies of the assemblage as a whole (e.g., Blonder et al., 2014; Butrim et al., 2022), the amount of deciduousness versus evergreen-ness at the site (Carvalho et al., 2021), and how different environmental forcings may have affected plant strategy and assembly (Butrim et al., 2022). Site-mean LMA estimates have also been used to compare the plant economics of multiple localities, and to investigate how environmental conditions could have affected them (Lowe et al., 2018; Butrim et al., 2022).

Reconstructions of LMA distributions have been used for many of the same types of interpretations—differences between LMA distribution curves have been interpreted to signify shifts in plant economic strategies (Lyson et al., 2019; Butrim et al., 2022); as responses to changes in temperature, rainfall, or atmospheric CO<sub>2</sub> (Roth-Nebelsick et al., 2017; Butrim and Royer, 2020); and as possible products of the deposition and fossilization process (Blonder et al., 2014). Beyond that, LMA distributions have often been used to assign fossil floras to biomes, by finding similarities between reconstructed fossil LMA distributions and the modern LMA distributions of floras selected to represent specific biomes (Royer et al., 2010; Flynn and Peppe, 2019; Allen et al., 2020; Baumgartner and Peppe, 2021; West et al., 2021; Wagner et al., 2023).

These site-level LMA interpretations are something of a paleobotanical novelty, especially when involving LMA distributions. While neobotanical studies have investigated the effects of climate on site-mean LMA (Wright et al., 2005) and examined community assembly through an LMA lens (Cornwell and Ackerly, 2009; Kraft and Ackerly, 2010; Paine et al., 2011; Wieczynski et al., 2021; Gomarasca et al., 2023), LMA distribution curves are rarely treated as free-standing attributes of sites. Moreover, the data that go into

these modern studies are fundamentally different from the data available in the paleobotanical record: modern studies typically include plant functional groups like herbs, which are rarely fossilized, and needle-leaved conifers, which have no reliable LMA proxy; often weight species by abundance (Wieczynski et al., 2021); constrain themselves to a limited number of habitat types or plant demographic stages (Kraft and Ackerly, 2010; Paine et al., 2011); or use global rather than local/in situ species-mean LMA values (Lamanna et al., 2014).

In practice, the use of site-level LMA, and particularly LMA distribution curves, is given far more explanatory weight in paleobotanical studies; currently, many of these methods are not well grounded in empirical neobotanical data. The strength of paleobotanical LMA reconstructions comes from the understanding that LMA, a trait shaped by physical and physiological factors, follows the principles of uniformitarianism especially well. Thus, for the continued use of site-level LMA as an important paleobotanical data point, it is critical that these relationships are supported by modern data. This is especially true because LMA can vary substantially at every level (Messier et al., 2017): a single plant can have leaves in its canopy with five times the LMA as at its base, the same species at one locality may have twice the mean LMA as at another (Messier et al., 2010), and yet the vast majority of species within two different forest biomes can have overlapping LMA ranges (Poorter et al., 2009). It is by no means a given that factors that coordinate LMA at one level will be impactful at another.

Here, we test the hypothesis that paleobotanical sitelevel interpretations of LMA are legitimate: that LMA distributions can accurately assign a flora to a biome and that shifts in LMA distribution can be linked to changes in climate, deciduousness, taxonomic composition, and/or depositional environment. By doing this, we seek to contextualize interpretations of site-level LMA and to create the support needed for the continued growth of this important fossil functional trait. We use extensive fossil and modern LMA data sets, curated such that all data are taken in the same way that paleobotanical LMA data are taken-sitebased, and restricted to woody, petiolate, non-monocot ("dicot"), angiosperm leaves. We first check that simple, and well-known correlations between species-mean LMA and various environmental factors are present in the modern data set, and where possible evaluate whether the same correlations can be seen in the fossil data set. We also investigate site-mean LMA correlations with climate in the modern data set and evaluate whether sites follow broadly the same trends as species. Finally, we analyze LMA distributions using a variety of multivariate techniques to investigate if and when differences between LMA distributions can be understood to reflect factors such as climate and taxonomic composition. Importantly, because we include both modern and fossil data sets, we can evaluate the influence of climatic and phylogenetic factors that may not be testable in the fossil record. Conversely, using the fossil data set, we can evaluate whether variables that cannot

be, or simply have not been, collected in the modern record—such as depositional environment or the leaf architectural characters used to delineate morphospecies—have significant impacts on reconstructed LMA results. Through careful analysis of this combined fossil and modern LMA data set, we build a better understanding of what LMA can tell us about plant communities and their environment.

## MATERIALS AND METHODS

#### Fossil data set

The fossil LMA data set was built via a literature search, last updated in May 2022, through all work citing the original petiole-width method paper by Royer et al. (2007). LMA data was included in the data set if it had morphospecies-mean values for ≥10 morphospecies at a given site. These criteria ensure that each included site could be used in analyses of LMA distribution and site-mean LMA. When available, age, depositional environment, mean annual temperature (MAT), mean annual precipitation (MAP), and GPS coordinates were collated for each site. Age was recorded to whatever specificity could be found in the literature; if only a range was provided, a suitable midpoint was chosen. Sites were assigned to coastal, fluvial, lacustrine, or mixed depositional environments. MAT and MAP estimates were derived through multiple methods, but when different options were available, we prioritized leaf physiognomic methods such as leaf margin analysis (Wilf, 1997) and CLAMP (Yang et al., 2015), which are often used in conjunction with LMA reconstructions. Whittaker biomes were assigned when both MAT and MAP estimates were available using the "ggbiome" package in R (Bagaria et al., 2022). CO<sub>2</sub> levels were estimated for each site where age was available using the LOESS curve built by Foster et al. (2017).

To evaluate the relationship between LMA and leaf architecture, we collected two types of data that represent how leaves fit within the bounds of leaf morphological diversity (morphospace). The first allowed a more granular construction of morphospace but could only be pursued for a subset of sites. For this method, we compiled leaf architectural characteristics for each morphospecies at a given site following the Manual of Leaf Architecture (Ellis et al., 2009). We used published morphospecies descriptions when available; otherwise, we entered characters based on photographs or plates. Many characters were unobtainable through these means, so for analysis we picked a suite of well-represented and easily extractable traits that cover most major categories in the Manual of Leaf Architecture: laminar length to width ratio, medial symmetry, base symmetry, lobation, tooth presence, margin type, apex angle, base angle, primary vein framework, major secondary vein framework, and intercostal tertiary vein fabric. In some cases, our data/image resolution was too low, or the preservation of the fossils too poor, to account for each

character state, so we lumped states into larger groups when necessary (Appendix S1: Table S1).

The second type of morphospace representation used was the trait combination type concept (TCT; Roth-Nebelsick et al., 2017). This can be considered a simple way of assigning morphospecies to a bin in morphospace (TCTs A-P) based on a series of dichotomies considering leaf lobation, leaf toothiness, pinnate or palmate primary venation, and looped or unlooped secondary venation. The simplicity of this method allowed us to include more morphospecies and to build easily comparable site-level descriptions of morphospace based on the relative frequency of TCTs at each site.

#### Modern data set

The modern LMA data set was built by manually searching through the list of all data sets included in the TRY plant trait data base (Kattge et al., 2020). Our criteria for data set inclusion were that LMA or its inverse, specific leaf area, were included (TRY TraitIDs: 4083, 3115, 3116, 3117) and that sampling represented a site rather than just a few targeted taxa. With these criteria, we obtained data from 12 data sets (Wright et al., 2004, 2007; Cavender-Bares et al., 2006; Poorter and Bongers, 2006; Swaine, 2007; Fyllas et al., 2009; Baraloto et al., 2010; Messier et al., 2010; Penuelas et al., 2010; Gonzalez-Akre et al., 2015; Kearsley et al., 2017; Wang et al., 2018; see Appendix S1: Table S2). Extensive data cleaning was required to standardize these disparate smaller data sets. Species names were aligned to the World Flora Online phylogenetic backbone (WFO, 2024) using the "WorldFlora" package in R (Kindt, 2020). Species that could not be easily located on the WFO backbone after a secondary manual search were removed. Non-dicot species were then omitted to best match the fossil data set. Plant growth form was either listed as a species character or was a data set property (e.g., the RAINFOR data set is entirely trees). Species listed as vines, graminoids, pteridophytes, herbs, epiphytes, hemiepiphytes, parasites, forbs, bamboo, geophytes, climbers, and succulents were omitted, leaving a variety of woody dicot forms. Leaf type was provided in some data sets, and needle and scale-leaved species were omitted. After applying these filters and then using the same 10-species minimum as for fossil sites, we evaluated each of the remaining sites and removed those that specifically focused on saplings or that were restricted to narrow taxonomic groups. The Digital Leaf Physiognomy (DiLP) data set, which is used as a basis for many paleoclimate reconstructions (Peppe et al., 2011), is not currently uploaded to TRY but meets the same criteria and was included in our analysis.

To include deciduousness as a factor in our analyses, we added leaf habit data to the modern data set because it was typically not recorded in the source data. A list of all data under TRY TraitID 37 (leaf phenology type) was downloaded and matched by species name to the species in our

modern LMA data set. We did not record leaf habit for species with multiple, conflicting matches or for difficult-to-classify semi-deciduous and semi-evergreen species.

To associate the modern sites with climatic variables, we downloaded the WorldClim (worldclim.org) geotiff map layers (Fick and Hijmans, 2017). These are high-resolution (30 arc seconds/~1 km<sup>2</sup>) gridded climate maps interpolated from a dense network of weather station data. We chose maps based on yearly averages from 1970-2000 of 19 bioclimatic variables, which include MAT, MAP, and various metrics of seasonality. We also downloaded a set of BIO-CLIM+ maps (chelsa-climate.org), which are similar in concept to the WorldClim maps, but represent more derived climatic variables that are further abstracted from the base weather station data (Brun et al., 2022). Eleven BIOCLIM+ maps provided yearly averages, including for climate variables with known site-level correlations with LMA (Wright et al., 2005), such as vapor pressure deficit (VPD) and surface downwelling shortwave radiation (RSDS).

Except for MAT and MAP, we used the gridded estimates extracted from the bioclimatic maps without modification. For MAT and MAP, we preferentially used the values reported from the TRY data sets, because these individually curated values were more responsive to variation in elevation. However, the gridded estimates were tightly correlated to the reported values (MAT: r = 0.99; MAP: r = 0.92), so when individual data sets did not report MAT or MAP, we were comfortable using the gridded estimates. As with the fossil sites, each modern site was assigned to a Whittaker biome using MAT and MAP.

## **Analysis**

All analyses were conducted in R version 4.0.2 (R Core Team, 2023). Species-mean LMA was log-normal distributed, so for any correlative (parametric) analysis we applied a log<sub>10</sub> transformation to all species-mean LMA values. Sitemean and site-distribution LMA values were calculated based on the mean log<sub>10</sub> transformed species-mean values for sites in our modern data set. For fossil sites a separate site-mean LMA regression based on untransformed specieslevel petiole-width and leaf-area measurements was used (Royer et al., 2007). By using this regression, we avoid compounding the error generated in each species-mean LMA reconstruction. We evaluated the distribution of each environmental variable for log normality as well and found that measures of precipitation also required a log<sub>10</sub> transformation for correlative analyses. Linear regressions correlating LMA with climatic variables were calculated with the "lm()" function in R (R Core Team, 2023).

To compare LMA distributions between sites, the set of species-mean LMA values at each site was converted into a Gaussian probability distribution between the minimum and maximum  $\log_{10}$  transformed LMA values of 0.65 and 2.90. These probability distributions were transformed into a distance matrix with the "philentropy" package (Drost, 2018)

using Jensen-Shannon divergence (Lin, 1991), a symmetrical distance metric that measures the distance between two probability distributions. Each site was then clustered using agglomerative hierarchical cluster analysis based on complete linkages ("hclust" in the "r stats" package; R Core Team, 2023) to create a dendrogram illustrating groups of sites with similar LMA distribution curves. The complete linkage method was chosen because it generally performs well with continuous functional data (Ferreira and Hitchcock, 2009) and produced more visually distinctive clusters than Ward's method, which also performs well with this type of data. These distinctive clusters were selected from the dendrogram, and the cluster membership of each site was used as a representation of the site's LMA distribution in subsequent analyses.

Nonmetric multidimensional scaling (NMDS) was used to illustrate whether LMA distribution clusters plotted in different areas of taxonomic space. We used the Raup-Crick dissimilarity metric for presence/absence data sets (Chase et al., 2011) from the "vegan" package (Oksanen et al., 2022) to build a distance matrix between all modern sites characterizing the dissimilarity of sites in terms of the presence/absence of taxa at the family level. Many families were quite site-specific, so to construct an ordination with low stress we included only sites that contained ≥15 families, and then excluded families that were not found in at least two sites. We ran NMDS on the trimmed dissimilarity matrix using the "metaMDS" function in the "vegan" package and used analysis of similarities (ANOSIM) to evaluate whether clusters grouped in statistically different sectors of the ordination.

With the species-level leaf architectural data that we compiled for the fossil data set, we investigated whether there are links between LMA and shifts in morphospace. We used principal coordinate analysis (PCoA) as the ordination method, and Gower dissimilarity to build the distance matrix (Gower, 1971; Podani, 1999; Laliberté et al., 2014). This combination is robust with data that has asymmetric binary options and a mix of binary, quantitative, and qualitative variables. We then used the "ordisurf" function in the "vegan" package to plot a smoothed contour surface for LMA and to measure how much variation in LMA could be explained by the ordinated morphospace. With our broader, site-level TCT data, we returned to NMDS to visualize how LMA distribution clusters plotted in leaf morphospace. We constructed a matrix of the abundance of each TCT at each site and then transformed it into a distance matrix using the Bray-Curtis dissimilarity metric, which is appropriate for species abundance data (McCune and Grace, 2002). As with the taxonomic data, we filtered out TCTs that could only be found at one site to increase the power of the ordination.

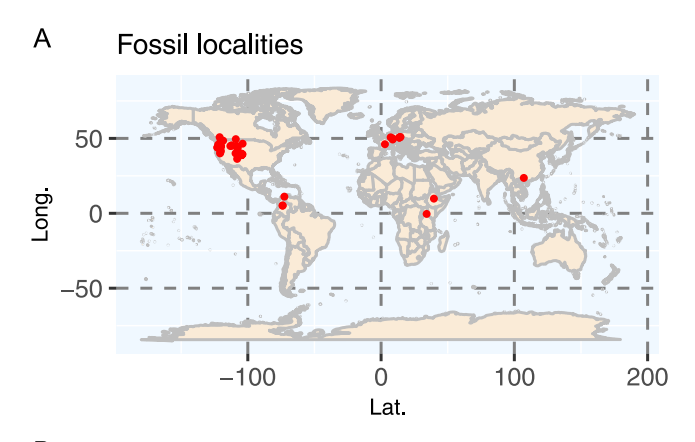
Finally, throughout our investigation, we evaluated the relationship between LMA distribution clusters and various quantitative and categorical variables. To identify how clusters differed, we used Tukey's HSD test through the "multcomp" package (Hothorn et al., 2008), which compares means between multiple groups, and the Mann-Whitney

*U*-test (Sokal and Rohlf, 2012), which compares medians between two groups.

## RESULTS

#### Data sets

After cleaning the data, the fossil LMA data set totaled 1209 morphospecies-site pairs (Appendix S1: Table S3), and 56 sites represented by ≥10 morphospecies (Appendix S1: Table S4). Over 75% of sites come from western North America (n = 43), but Europe (8), South America (2), Africa (2), and Asia (1) are also represented (Figure 1A). A wide range of climate variation is captured, with estimated MAT ranging from 7°C to 28°C and MAP ranging from ~600 to >3000 mm/yr. This translates to coverage of the tropical rainforest, tropical seasonal forest/savanna, temperate rainforest, temperate seasonal forest, and woodland/shrubland Whittaker biomes (Appendix S2), leaving the desert, grassland, boreal forest, and tundra biomes unrepresented. Temporally, much of angiosperm evolutionary history is captured, with sites dating to between 105 and 18 mya. Finally, most fossil sites were deposited either in fluvial (n = 30) or lacustrine (22) environments, with only a few sites from coastal (2) or mixed (2) depositional settings. Specific



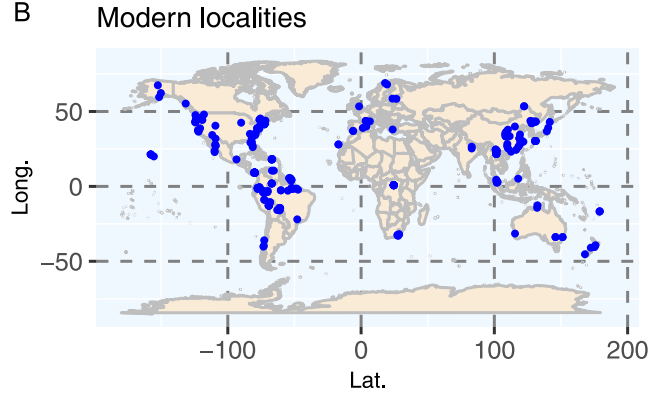


**FIGURE 1** Map of (A) fossil localities and (B) modern localities represented by  $\geq 10$  species/morphospecies with measurable leaf mass per area.

environmental and other site-level data are presented in Appendix S1: Table S4.

The modern LMA data set totaled 7073 species-site pairs (Appendix S1: Table S5) from 255 sites after data cleaning (Appendix S1: Table S6). Site coverage is excellent, with locations on every continent but Antarctica (Figure 1B), and from every Whittaker biome (Appendix S2). Thirty gridded bioclimatic and BIOCLIM+ variables were extracted for each modern site; MAT ranges from -9°C to 31°C, and MAP ranges from 120 to 4725 mm/yr (for detailed climatic results, see Appendix S1: Table S6). As with the fossil data set, the tropical and temperate forest biomes and the woodland/shrubland biome are the best represented. Several sites do not fall within the standard boundaries of the Whittaker biomes; many of these anomalous sites come from mountainous parts of regions with high rainfall, where high elevations have dropped temperatures below the local average.

## Species and site-level climate correlations

MAT and MAP were the only variables that could be tested against LMA across both modern and fossil data sets. In the modern data set, MAT has a positive correlation with LMA at both the species (n = 7073, r = 0.29, P < 0.001; Figure 2A) and the site (n = 255, r = 0.43, P < 0.001) level. In the fossil data set, the correlation between MAT and LMA is negative at the species level (n = 1107, r = -0.12, P < 0.001), and not statistically significant at the site level (n = 50, r = -0.13, P = 0.36). Correlations with MAP are weaker and similarly contradictory. Among modern species (n = 7073, r = 0.17, P < 0.001; Figure 2B) and sites (n = 255, r = 0.12, P < 0.001) the correlation is positive. But in the fossil data set the correlation is negative at the species level (n = 898, r = -0.22, P < 0.001) and nonsignificant at the site level (n = 36, r = 0.20, P = 0.24). Because the fossil data set spans a narrower range of temperature and precipitation than the modern data set, we retested the modern MAT and MAP correlations using the same restricted climate bounds. Under these constraints, the correlation at the site level (n = 185 sites) is slightly weaker but still positive for MAT (r = 0.33, P < 0.001) and is stronger for MAP (r = 0.19, P = 0.01).

Atmospheric CO<sub>2</sub> could be tested only in the fossil data set, because the modern data set does not capture substantial CO<sub>2</sub> variance. With the caveat that the paleo-CO<sub>2</sub> data has the largest potential for error among our climate variables, due to both proxy imprecision (Foster et al., 2017) and inaccuracies in dating the fossil sites, we saw a minor, but significant, positive correlation between CO<sub>2</sub> and LMA at the species level (n = 1199, r = 0.11, P < 0.001; Figure 2C) and no significant correlation at the site level (n = 55, r = 0.23, P = 0.08).

The remaining climatic variables could be tested only in the modern data set. Among 30 gridded climate variables, 25 are significantly correlated with LMA at the site level and 29 are significantly correlated at the species level (Appendix S1: Table S7). Three of the variables most strongly correlated with site-mean LMA are surface downwelling

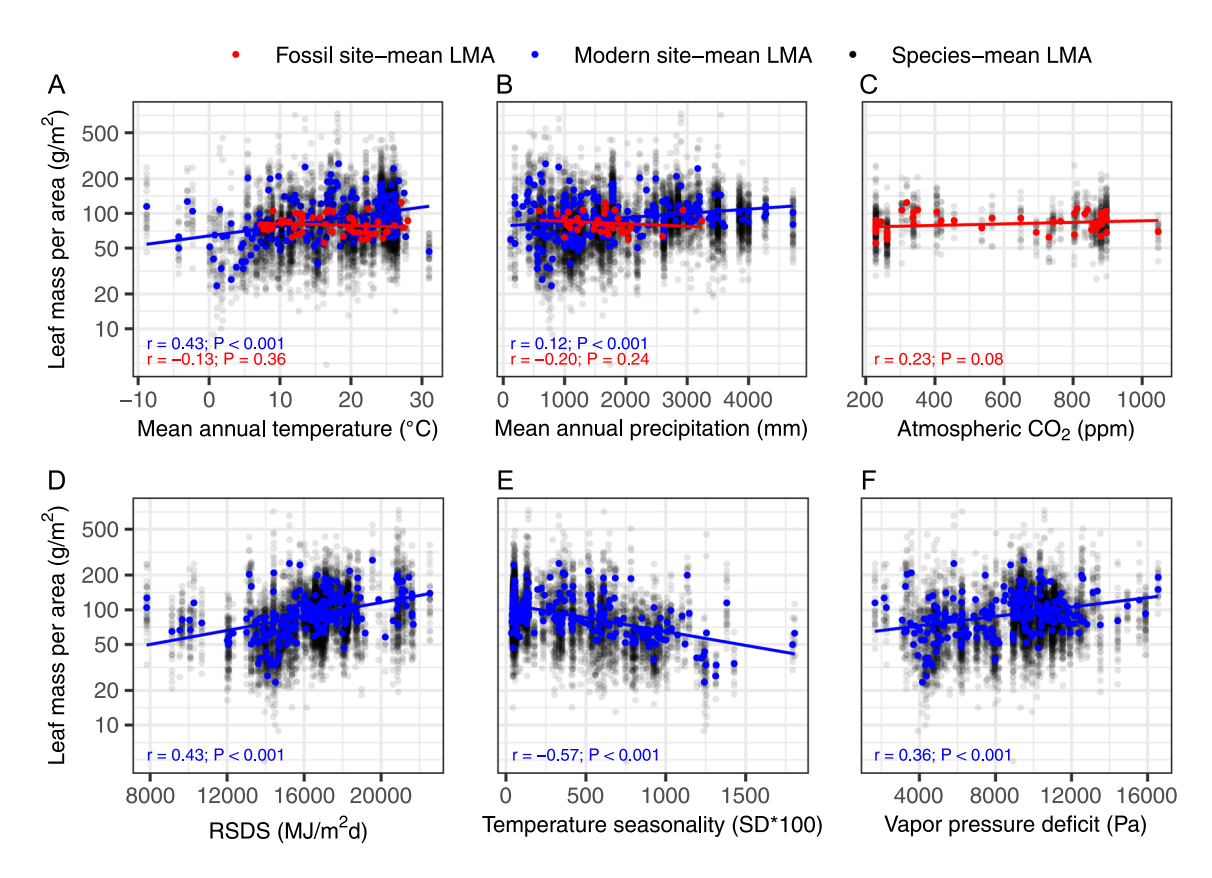


FIGURE 2 Linear regressions with site-mean leaf mass per area (LMA) as a function of (A) mean annual temperature, (B) mean annual precipitation, (C) atmospheric CO<sub>2</sub>, (D) surface downwelling surface radiation (RSDS), (E) temperature seasonality, and (F) vapor pressure deficit. Blue lines represent modern site-mean LMA regressions, blue dots represent individual modern site-means, red lines represent fossil site-mean LMA regressions, red dots represent individual fossil site-means, and gray dots represent individual species-mean LMA values.

shortwave radiation (RSDS; n = 255, r = 0.43, P < 0.001; Figure 2D), temperature seasonality (n = 251, r = -0.57, P < 0.001; Figure 2E), and vapor pressure deficit (VPD; n = 255, r = 0.36, P < 0.001; Figure 2F). We focus on these three variables because they have comparatively low levels of covariance among themselves (r = 0.55-0.73) but are still among the most strongly correlated with LMA (Appendix S1: Table S8). We tested the addition of a quadratic factor to regressions between site-mean LMA and these variables but found no significant improvement over the linear regressions (Appendix S3).

#### Distribution-level climate correlations

Agglomerative hierarchical cluster analysis with complete linkage produced a dendrogram with seven natural clusters (Figure 3A). The distribution curves within each cluster have a general character, which can be described as a combination of the height of the typical curve's peak (low, middle, or upper), and where the median of the curve falls along the LMA x-axis (leftmost to rightmost; Figure 3B). Hence, from left to right: "middle leftmost" (pink; n = 11 sites), "low left" (blue; n = 41), "middle left" (green; n = 66), "middle right" (purple; n = 74), "low right" (red; n = 89),

"upper right" (brown; n = 3), and "middle rightmost" (orange; n = 27). In other words, the site-mean LMA within each cluster rises from "leftmost" to "rightmost," and the variance in species-mean LMA of sites decreases from "low" to "middle" to "upper" (Appendix S4). The three earliest-diverging clusters on the dendrogram represent the "extreme" LMA distributions ("middle leftmost," "middle rightmost," and "upper right"), consist of relatively fewer sites, and have not yet been found in the fossil record. The four later-diverging clusters ("low left," "middle left," "middle right," and "low right") consist of more sites, are represented in the fossil record, and have the four most central distributions along the x-axis.

Modern sites from different distribution clusters typically experience different combinations of climate variables. From left to right, or as site-mean LMA increases, sites from the "middle leftmost," "low left," "middle left," and "middle right" clusters increase in average MAT, MAP, RSDS, and VPD, and decrease in average temperature seasonality (Figure 4). Tukey HSD tests show some variation in whether there are significant differences among the four clusters, but for each of these climate variables, at minimum the bracketing "middle leftmost" and "middle right" clusters are significantly different. Further to the right, as LMA increases, trends for all climate variables level off or reverse; climate values for the "low right" cluster are

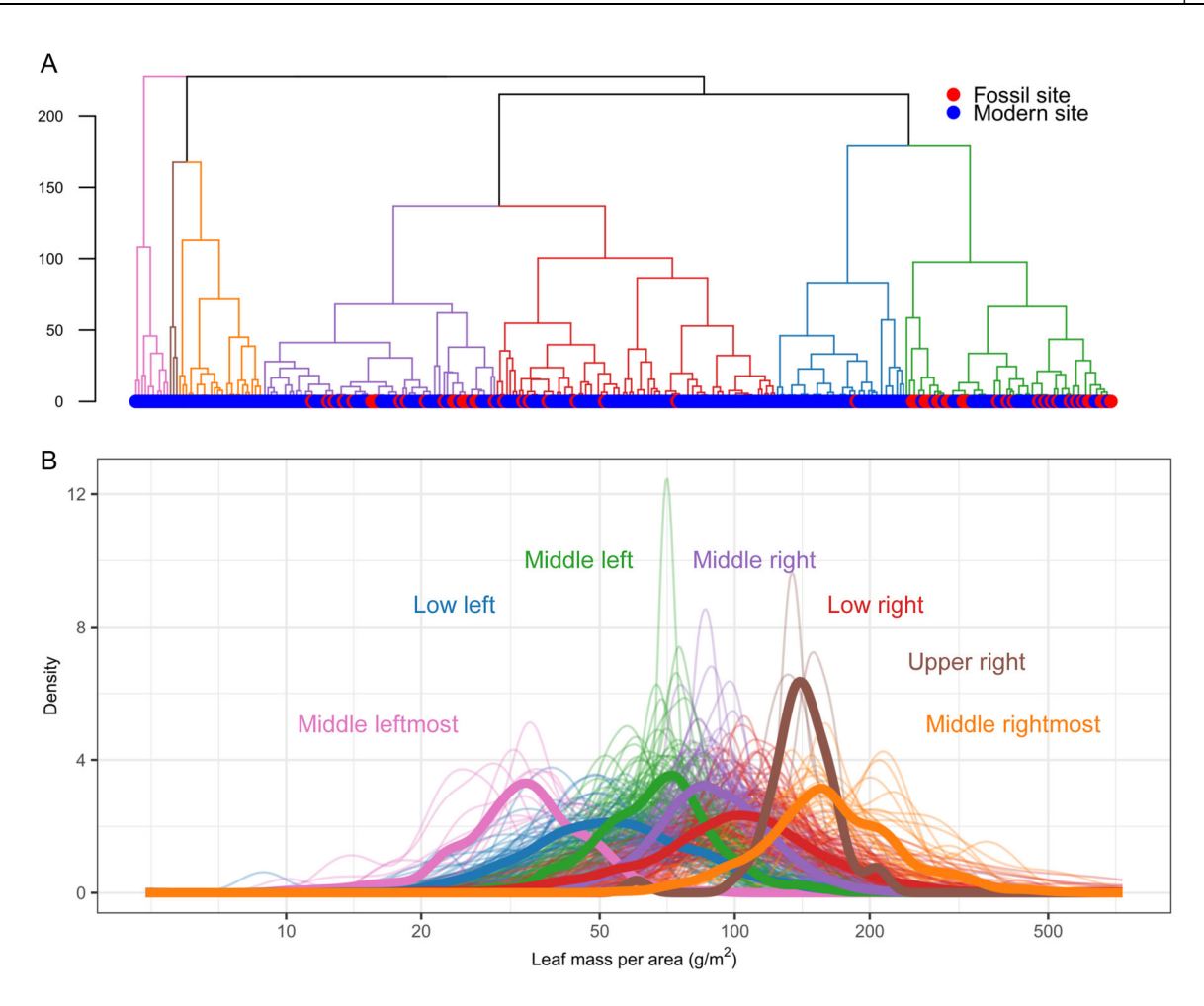


FIGURE 3 Visualizations of leaf mass per area (LMA) distributions. (A) Dendrogram representing the results of agglomerative hierarchical clustering on the LMA distributions of fossil and modern sites. The first seven clusters to diverge are highlighted by different coloration along their branches. At the base of the dendrogram, red dots represent fossil sites and blue dots represent modern sites (note that fossil sites appear in only four of the seven clusters). (B) Probability density functions of LMA distributions. Colors of lines correspond to colors on the dendrogram. Thin lines indicate LMA distributions of individual sites and the seven thick lines represent the combined distribution of every site within each of the seven colored clusters: "middle leftmost" (pink), "low left" (blue), "middle left" (green), "middle right" (purple), "low right" (red), "upper right" (brown), and "middle rightmost" (orange).

either indistinguishable from the adjacent "middle right" cluster (MAT, RSDS, temperature seasonality, VPD) or resemble more closely those of the "middle left" cluster (MAP). Even further to the right, among sites with the highest LMA values, the poorly represented "upper right" and "middle rightmost" clusters are indistinguishable from all but the "middle leftmost" and "low left" clusters.

In the fossil record, sites are concentrated in the "middle left" (n=28) and "middle right" (n=20) clusters, which have similarly shaped, fairly narrow distributions, but are respectively centered around lower and higher median LMA values. The "low left" (n=1) and the "low right" (n=7) clusters, characterized by wider and more even distributions, are also represented in the fossil record. The "middle left," "middle right," and "low left" clusters can be significantly differentiated by climate (Figure 4). Sites from the "middle left" cluster tend to be cooler, drier, and more seasonal than sites from the "middle right" cluster, while sites from the "low left" cluster tend to be even more cool and seasonal. The "low right" cluster cannot be easily differentiated from the climates of

either the "middle left" or "middle right" clusters but tends to most closely resemble "middle left."

To evaluate the significance of multivariate relationships between climate and LMA distribution clusters, we performed a principal component analysis using all 30 gridded climate variables (Appendix S5). The first and second principal components (PC1 and PC2) explain 71% of the climatic variance among the sites; however, ellipses plotted around the centroids of each LMA distribution cluster reveal significant overlap between most clusters, particularly along PC2. As observed in the univariate tests, the "middle left" and "low right" clusters have a high degree of similarity, while the "low left," "middle left," and "middle right" clusters are progressively staggered along PC1, an axis that runs nearly parallel to the temperature seasonality vector.

We also examined how clusters were distributed across the Whittaker biomes (Figure 5). There are apparent differences between biomes—for example, the tropical rainforest biome mostly consists of sites that fall into the high LMA "middle right" and "low right" clusters, while the

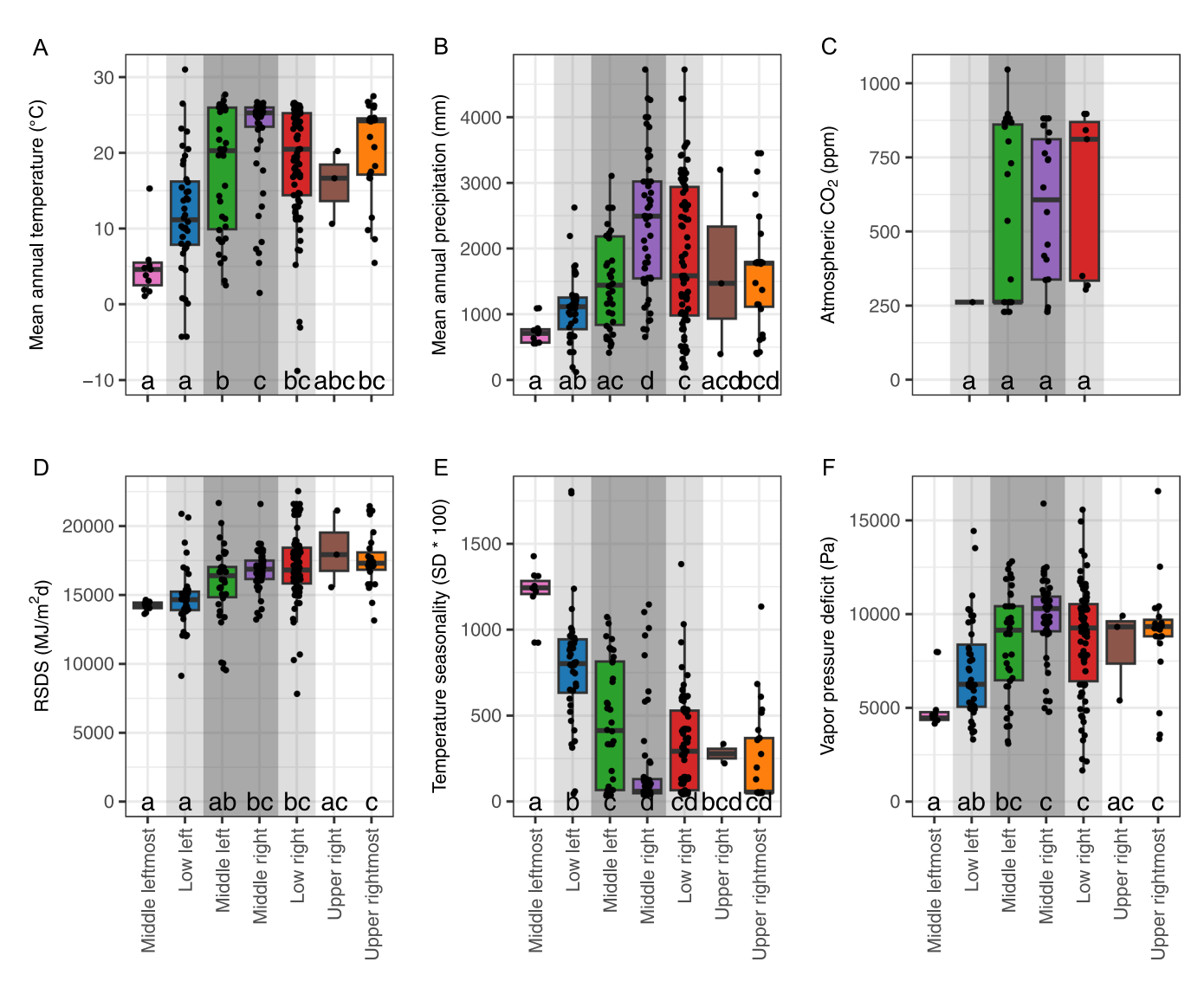


FIGURE 4 Box and whisker plots showing the relationship between modern leaf mass per area (LMA) distribution clusters and six climatic variables: (A) mean annual temperature, (B) mean annual precipitation, (C) atmospheric CO<sub>2</sub>, (D) surface downwelling shortwave radiation (RSDS), (E) temperature seasonality, and (F) vapor pressure deficit. Dots represent the individual sites that make up each cluster. Box boundaries represent the first and third quartiles, with the median represented by the line inside the box. Tukey HSD test groups are displayed at the bottom of each panel; clusters that do not share letters are significantly different from one another. Colors signify which cluster the box belongs to. The shaded region on each panel highlights the clusters that have been found in the fossil record; the darker shaded region highlights the two clusters in which fossil sites are most likely to be found.

boreal forest biome mostly consists of sites from the low LMA "middle leftmost" and "low left" clusters. At the same time, all seven biomes represented by four sites or more include a site from at least four different clusters.

## LMA and taxonomic composition

We investigated whether there was an identifiable connection between LMA distribution cluster and the taxonomic composition of a site. In the modern data set, 186 plant families are represented, but after trimming the data set for NMDS and ANOSIM, 133 families across 83 sites remained. ANOSIM indicates significant taxonomic differences among clusters (r = 0.16, P = 0.001), which can be seen on the

NMDS (Figure 6). Sites from the "low left," "middle left," and "middle right" clusters occupy similar spaces along NMDS axis 2, while sites from the "low right" cluster tend to plot below the rest. On NMDS axis 1, sites from the "low left," "middle left," and "middle right" clusters plot progressively further to the left. Sites from the "low right" cluster occupy most of the width of NMDS axis 1 with a centroid that falls most closely to the centroid of the "middle left" cluster.

## LMA and deciduousness

Deciduousness was negatively correlated with LMA. Using the modern data set, deciduousness drops across the range

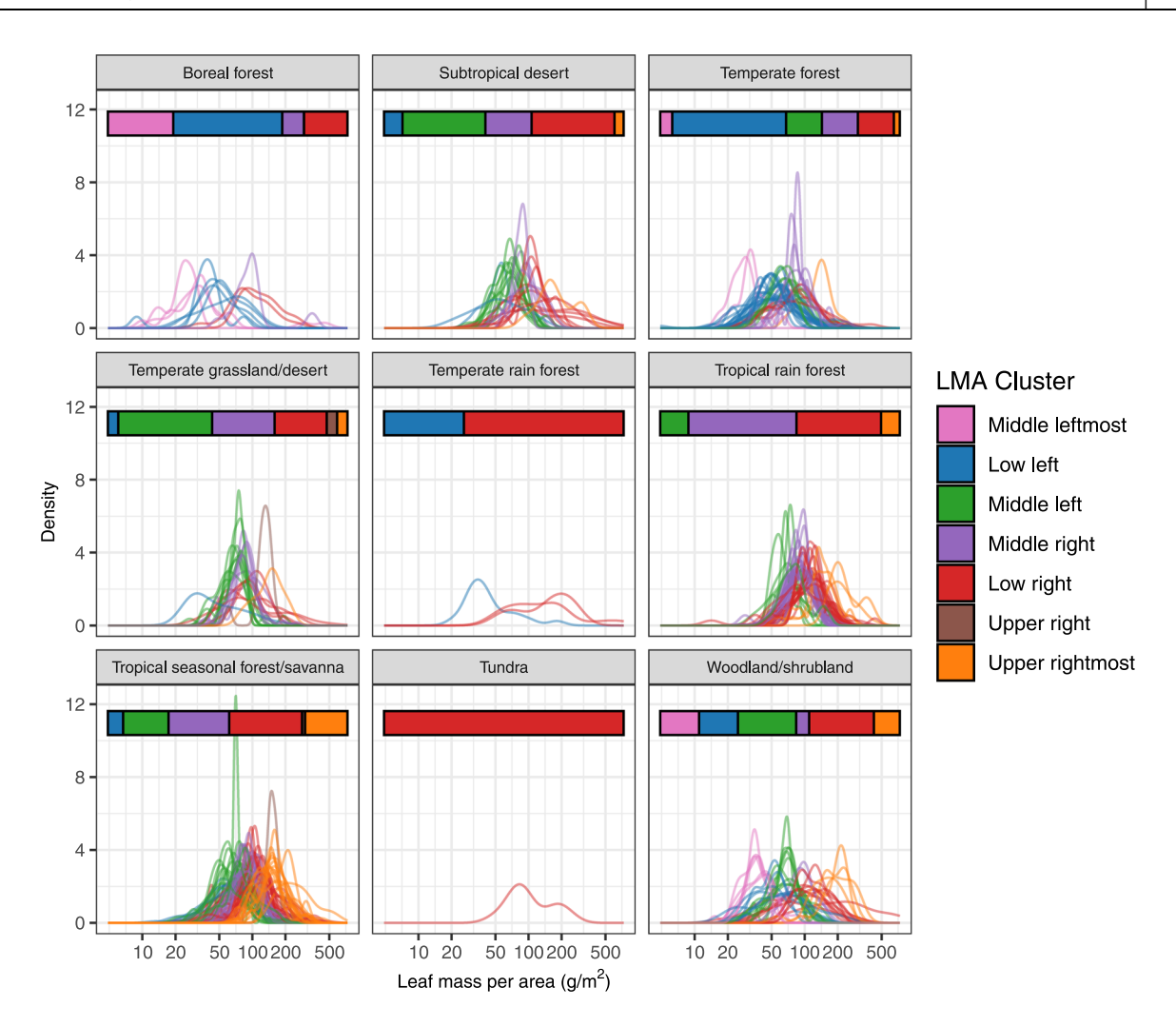


FIGURE 5 Relationship between modern leaf mass per area (LMA) distributions and Whittaker biomes. Each panel represents a single Whittaker biome. At the top of each panel is a colored bar graph that shows the proportion of sites from that biome that belong to each of the LMA distribution clusters. Below the bar graph, probability distribution functions represent the LMA distributions of individual sites belonging to the biome, similarly color-coded to the seven clusters. Proportions are different across biomes, but the four most common clusters, "low left," "middle left," "middle right," and "low right," are found in every biome represented by more than three sites.

of LMA observed in the fossil record, from ~78% of species deciduous at the lowest levels of fossil LMA (22–36 g/m²) to ~10% of species deciduous at the highest (162–269 g/m²; Figure 7A). Deciduousness seems to differentiate clusters as well (Figure 7B). Distribution curves that fall on the low end of the LMA axis (e.g., "middle leftmost" and "low left") have by far the highest proportion of deciduous species, while those on the high end (e.g., "middle right" and "middle rightmost") have the lowest. The "low right" cluster cannot be statistically differentiated from the "middle right" or "middle left" clusters.

## LMA and morphospace

The other broad factor that we investigated in association with LMA was leaf architectural morphospace. Our detailed multivariate analysis was based on observations from 351 fossil morphospecies-site pairs (Appendix S1: Table S1).

We plotted contour lines for reconstructed LMA on top of a principal coordinate ordination and found that 8.15% of the variation in LMA can be explained by morphospace (Figure 8A). At the univariate level, among the 10 characters and 38 character states evaluated, the only significant LMA differences are between morphospecies with dentate teeth (pointed teeth extending perpendicularly from the leaf margin) vs. crenate teeth (smoothly rounded teeth) and between morphospecies with acute (<90°) vs. obtuse (90°–180°) base angles (Appendix S6).

Trait combination types (TCTs) are also undifferentiated in terms of species-mean LMA. We were able to assign TCTs to 575 fossil morphospecies-site pairs from 28 sites. Twelve TCTs occur in at least two sites, and a Tukey HSD test showed no significant differences in LMA among them (Appendix S7). However, NMDS and ANOSIM based on TCT abundance at each site indicate that there is a significant correlation between LMA cluster and where sites plot in TCT morphospace (r = 0.22; P = 0.009; Figure 8B).

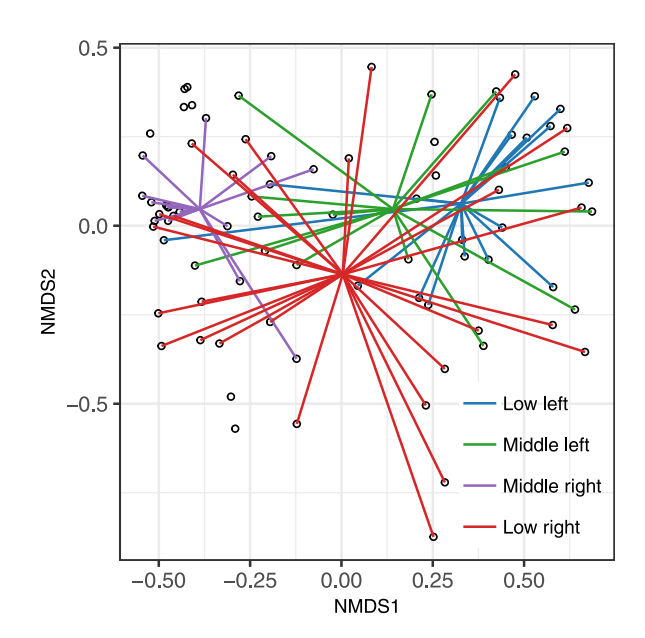


FIGURE 6 Nonmetric multidimensional scaling (NMDS) ordination illustrating how modern leaf mass per area (LMA) distribution clusters are spread across taxonomic space. Each point is a modern site, placed in the ordination space by the presence or absence of different plant families. Points are connected by spider-plots, which radiate from the centroid of each LMA distribution cluster to every site belonging to that cluster. Unconnected points come from clusters represented by two or fewer sites.

# LMA and depositional environment

Fossil sites are dominated by fluvial and lacustrine depositional environments. Fluvial sites have significantly lower site-mean LMA than lacustrine sites (77 g/m $^2$  vs. 87 g/m $^2$ ; Mann-Whitney U-test P = 0.03). However, fluvial and lacustrine sites cannot be differentiated by LMA distribution cluster (Figure 9). The "middle left" and "middle right" clusters are well represented in both environments, and a chi-square test reveals no evidence of independence (P = 0.49). Sample sizes for mixed and coastal depositional environments are too low to draw any conclusions.

## **DISCUSSION**

## Species- and site-mean LMA and climate

Well-supported correlations can reveal which factors drive LMA variation at global scales. The correlations between LMA and climate in our modern data set broadly align with other global-scale studies of modern LMA. Positive correlations of LMA with irradiation and water availability, and negative correlations of LMA with seasonality, are well established (Niinemets, 2001; Poorter et al., 2009; Bartlett et al., 2012) and map closely to the strong correlations that we found of species- and site-mean LMA with RSDS, VPD, and temperature seasonality. The positive correlation between LMA and temperature is also supported in the literature (e.g., Wright et al., 2004, 2005;

Poorter et al., 2009), although some studies found no relationship (Pinho et al., 2021) or a negative relationship (e.g., Mason et al., 2011; Swenson et al., 2012; Simpson et al., 2016; Bruelheide et al., 2018; Wieczynski et al., 2019). Our finding of a net-positive correlation between LMA and MAP contradicts the negative correlation found in most other global-scale studies (Wright et al., 2005; Moles et al., 2014); however, MAP correlations are consistently weak and are strongly influenced by the relative representation of deciduous and evergreen species within the data set (Wright et al., 2005). Our results may simply reflect a greater representation of deciduous species in our data set after the removal of evergreen gymnosperms.

Comparable correlations made in the fossil data set are limited to MAT and MAP and suggest a mismatch between the fossil and modern data sets. Both variables are positively correlated with modern LMA and negatively correlated with fossil LMA. Despite this discrepancy, the universalistic hypothesis—that the factors affecting LMA today are the same as those that affected LMA in the past—probably still holds. The inconsistent correlation between LMA and MAT and the general weakness of the correlation between LMA and MAP suggest that neither should be considered a primary global driver of LMA. Nor should we treat a variable like atmospheric CO<sub>2</sub> as a primary driver, because beyond the large error inherent to paleo-CO<sub>2</sub> reconstructions (Royer et al., 2001), the difficulty of identifying a consistent CO2 signal in labcontrolled modern experiments (Peterson et al., 1999; Norby et al., 2003; Gutiérrez et al., 2009; Poorter et al., 2009) suggests yet another variable with a subordinate role in filtering LMA.

Instead, because factors like temperature seasonality, irradiation, and water availability are most strongly correlated with LMA in our modern data set, we suggest that they are more appropriate for consideration when interpreting fossil LMA. Indeed, temperature seasonality may help explain the discrepancy between the fossil and modern correlations with MAT, given that the fossil data set contains non-analog climates in which the relationship between seasonality and MAT was disjointed, including the hothouse early Eocene, when forest ecosystems thrived within a warm but photically seasonal Arctic (West et al., 2020). Unfortunately, these variables cannot be reconstructed reliably in the geologic record (Peppe et al., 2010, 2018). In the absence of precise reconstructions, it is important that the modern LMA data set act as a strong reference point. Where MAT and MAP had inconsistent correlations even across modern studies, correlations between LMA and temperature seasonality, RSDS, and VPD are consistent, and thus likely remain consistent through geologic time as well.

## LMA distributions

Our analysis of LMA distributions reaffirms the importance of environmental factors in organizing LMA assembly and adds a new dimension to our understanding of their impact.

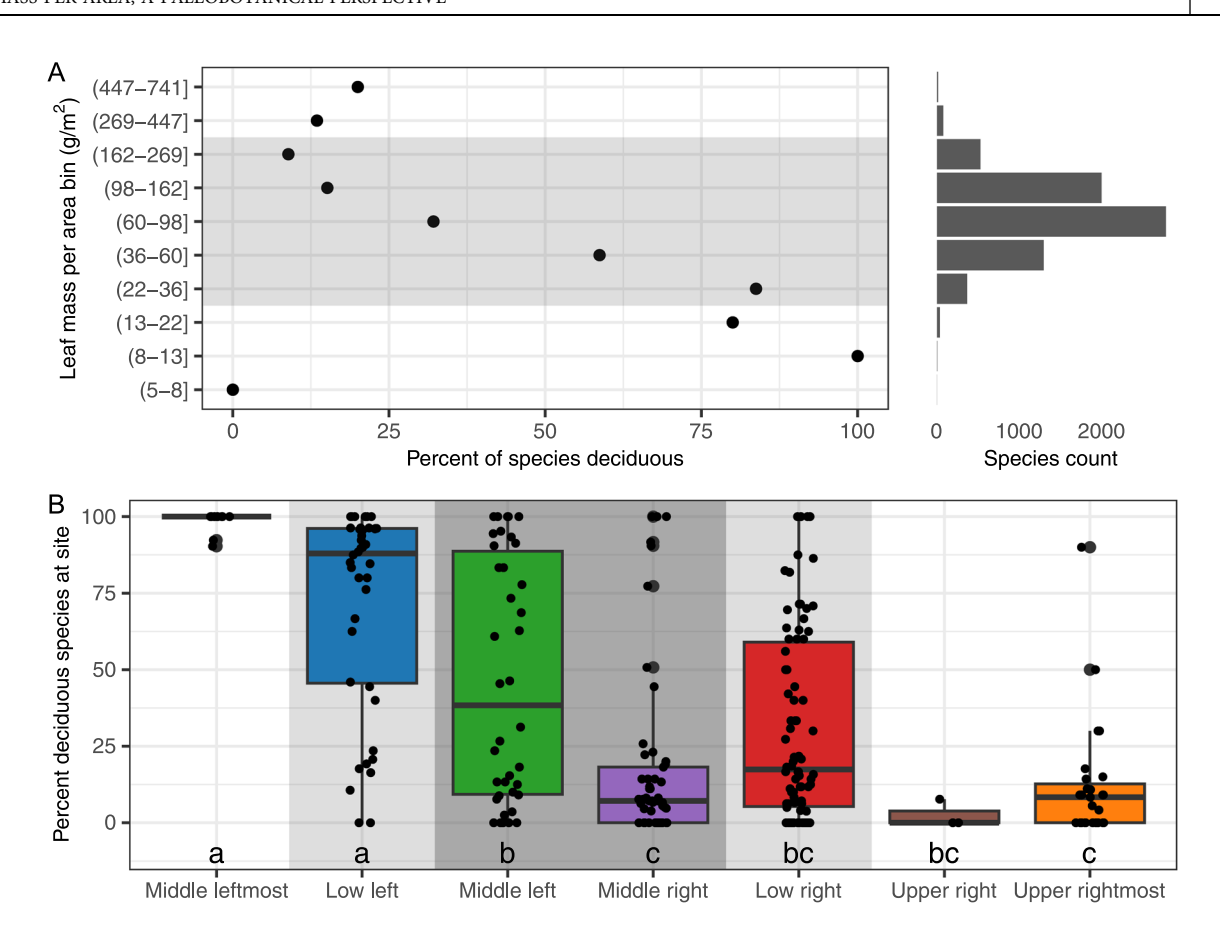


FIGURE 7 Relationship between deciduousness and modern leaf mass per area (LMA). (A) Species-mean LMA and deciduousness. The range of LMA  $(5-741 \text{ g/m}^2)$  represented in our data set is broken up into 10 even bins in  $\log_{10}$  space. The shaded region highlights the bins that fossil morphospecies are found in. (B) Box and whisker plots showing the relationship between LMA distribution clusters and deciduousness. Box boundaries represent the first and third quartiles, with the median represented by the line inside the box. Tukey HSD test groups are displayed at the bottom of each panel; clusters that do not share letters are significantly different from one another. Colors signify which cluster the box belongs to. The shaded region highlights the clusters that have been found in the fossil record, with darker shading showing the two clusters in which fossil sites are most likely to be found.

The seven LMA clusters created by our hierarchical clustering analysis of site-level LMA distributions are differentiated by both mean and evenness (Figure 3). Our naming scheme reflects this; from leftmost to rightmost, the clusters traverse the spectrum of what is essentially site-mean LMA, while from upper to lower, clusters are differentiated by whether they have narrower ranges with higher peaks (low evenness) or wider ranges with lower peaks (high evenness). Divided into these two axes, our results show that while site-mean LMA is the aspect of LMA distribution most responsive to climate, evenness can mask some of that response.

The two clusters with the lowest LMA and thus the fastest leaf economic strategies, "middle leftmost" and "low left," are the most climatically distinct, with sites typically found in comparatively cooler and drier environments with harsher winters. The remaining clusters are less differentiated from one another, but a site from the "middle left" cluster is more likely to come from a cooler, drier, and more seasonal climate than a site from the "middle right" cluster. This trend of increasing temperature, precipitation, and equability as site-mean LMA increases ends at the "low

right" cluster, which includes sites from a much wider range of climates, making it climatically indistinguishable from either the "middle left" or the "middle right" clusters. A similar pattern is observed in multivariate climate space (Appendix S5). While the "low right" cluster, with its high site-mean LMA, suggests slow leaf economic strategies compared to the "middle left" and "middle right" clusters, its higher evenness also suggests a lack of environmental filtering that could explain the absence of any specific climate association with the cluster. Thus, the evenness seen in sites from the "low right" cluster may in fact be a recognizable signal that a high site-mean LMA does not reflect a direct response to climate.

Despite significant climatic differentiation between some clusters, our findings suggest that LMA distributions have little power in predicting relative climate differences between individual fossil localities. Fossil sites are mostly found in three clusters: "middle left," "middle right," and "low right." As established, the "low right" cluster does not have a clear climate signal, and while the set of climatic values expressed within the "middle left" and "middle right" clusters are distinct, there is a significant amount of overlap

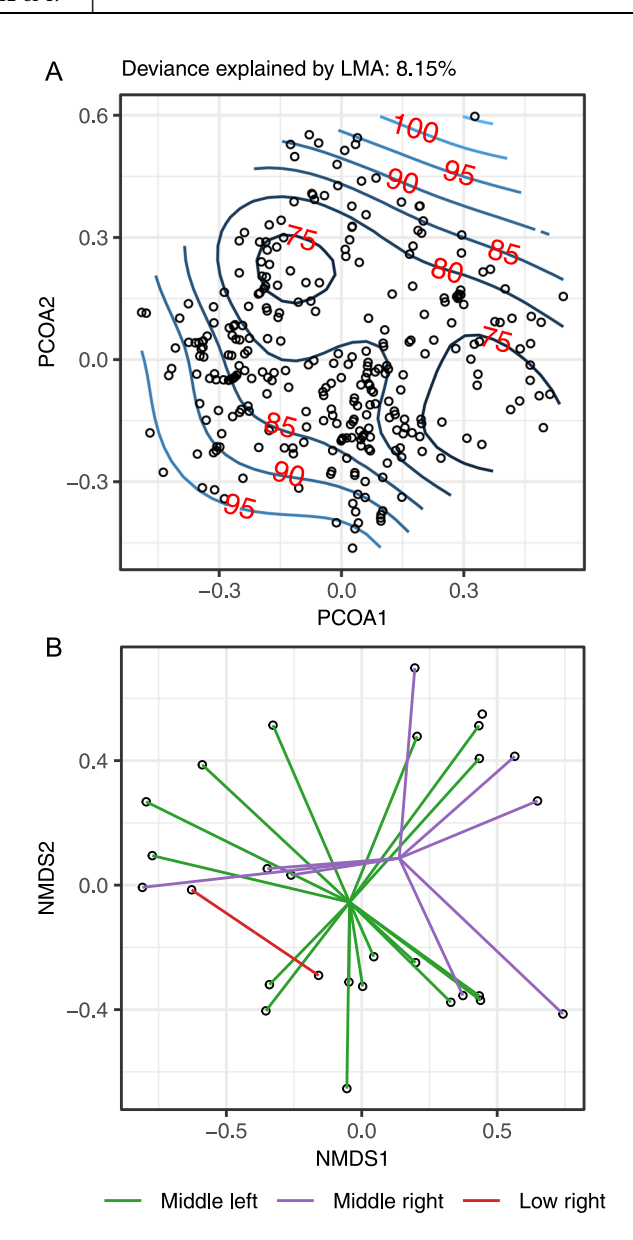


FIGURE 8 Relationship between reconstructed leaf mass per area (LMA) and morphospace. (A) A principal coordinate analysis showing morphospace based on leaf architectural characters. Each dot is a morphospecies from the fossil data set. The red contour lines represent the general trend of LMA across this plane of morphospace—from the inside out, LMA tends to increase. (B) Nonmetric multidimensional scaling (NMDS) ordination illustrating how LMA distribution clusters are spread across morphospace based on trait combination types (TCTs). Each point is a fossil site, placed in the ordination space by the proportion of each TCT at the site. Points are connected by spider-plots, which radiate from the centroid of each LMA distribution cluster to every site that belongs to that cluster. Unconnected points come from clusters represented by two or fewer sites.

among individual sites, regardless of which climatic variable is examined (Figure 4; see Appendix S5). Reconstructions of paleoclimate further emphasize the unreliability of using LMA distributions to estimate climate: the median estimated MAT of fossil sites from the ostensibly cooler "middle left" cluster is 19.2°C, four degrees higher than the

15.1°C estimated for fossil sites from the "middle right" cluster.

By extension, LMA distributions should not be used to place localities into biomes. MAT and MAP delineate the Whittaker biomes, and the fact that they cannot be confidently differentiated across the three main fossil clusters suggests that biomes will fare similarly. Indeed, none of the Whittaker biomes can be matched with high confidence to any of the clusters (Figure 5). Even when biomes are weighted toward a specific cluster, there is enough variation that sites from most of the other clusters can be found as well. In other words, while some biome types may be characterized by certain distribution types, the distributions lose their predictive power at the scale of an individual locality.

Our correlation analyses of LMA distributions versus non-climate factors further emphasize the difficulty of attributing shifts in LMA distribution to climate. For instance, LMA has a phylogenetic signal at the species level (Flores et al., 2014; Anderegg, 2023), and our results show that at the site level, LMA distributions are correlated with the taxonomic composition of a locality. The spread of the clusters in taxonomic space is similar to their spread in climate space, where the "low left," "middle left," and "middle right" clusters plot in succession along one axis while being almost entirely encircled by the area of taxonomic space occupied by the "low right" cluster (Figure 6). It should be noted that the methods used to create taxonomic space only incorporate taxonomy at the family level, and that to derive a low-stress ordination we removed low-abundance families from the analysis, resulting in a data set biased toward ubiquitous families that may not be characteristic of any specific flora. Still, our results show that the two clusters most commonly found in the fossil record can be differentiated by taxonomic composition. This makes it difficult to confidently attribute shifts in LMA distribution to climate if there is accompanying taxonomic turnover, such as in the aftermath of the end-Cretaceous mass extinction (e.g., Blonder et al., 2014; Butrim et al., 2022) or during the Paleocene-Eocene Thermal Maximum (e.g., Currano et al., 2008). At the same time, the similarity of the patterns in LMA distribution found in both taxonomic and climate space suggests that all three are inherently coordinated.

Deciduousness differentiates sites by LMA distribution in a similar fashion. Again, the "low right" cluster is indistinguishable from either the "middle left" or the "middle right" cluster (Figure 7B). And again, the "low left," "middle left," and "middle right" clusters are distinct from one another, progressively trending toward less deciduousness as LMA increases. This is consistent with the climate gradient associated with these three clusters and the close positive correlation between LMA and leaf life span, further suggesting that climate, taxonomic composition, and leaf habit may have confounding effects on LMA distribution. Unfortunately, LMA distributions do not provide a firm basis for estimating site deciduousness. While sites from the lower LMA "middle left" cluster are significantly more deciduous than sites from the higher LMA "middle right" cluster, there

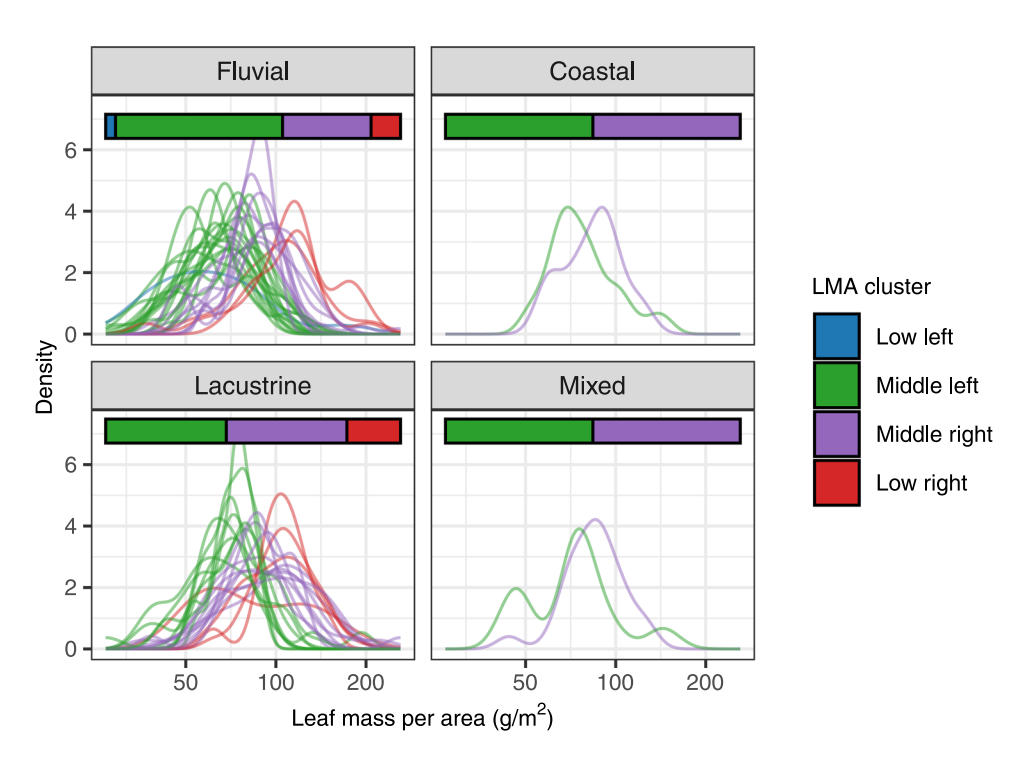


FIGURE 9 Relationship between reconstructed leaf mass per area (LMA) distribution clusters and depositional environment. Each panel represents an individual depositional environment. At the top of each panel is a colored bar graph that shows the proportion of sites from that depositional environment that belong to each of the LMA distribution clusters. Below the bar graph, probability distribution functions represent the LMA distributions of individual fossil sites coming from the depositional environment.

is non-negligible overlap at the individual site level (Figure 7B). Because sites with both 0% and 100% deciduousness are found in all clusters represented in the fossil record, fossil LMA distributions should not be used to determine whether deciduous or evergreen species dominate.

Considering the interwoven influence of climate, phylogenetics, and deciduousness on LMA distribution, it is important to recognize other factors that could not be assessed in our data set but may also play a role in determining viable leaf economic strategies. Disturbance regime (Herben et al., 2018; but see Haber et al., 2020), soil characteristics (Wright et al., 2002; Ordoñez et al., 2009), nutrient availability (Wright et al., 2002), and herbivory pressure (Hanley et al., 2007) all have influences on species-level LMA that could translate to LMA distribution but require specialized and laborious documentation to record. Documenting these factors in the fossil record is even more difficult, if not impossible. Similarly, factors affecting individual plants, or even leaves, could alter LMA distributions and are difficult to impossible to reconstruct from fossils. These include life history stage (Adler et al., 2014), canopy position (Cheesman et al., 2020), plant height (Coble and Cavaleri, 2015), and the time of year the leaf dropped (Reich et al., 1991).

# Fossil LMA aspects

Finally, our fossil data set enables new analyses of data typically only recorded in association with fossil leaves. Leaf architectural traits are often recorded by paleobotanists when sorting fossil leaves into morphospecies (Hickey, 1977; Johnson, 2002; Roth-Nebelsick et al., 2017), but the functional value of many of these traits is uncertain.

Morphospace captures simultaneous variance in leaf shape, size, and vein architecture (Stiles et al., 2020) but is only weakly correlated with LMA (Figure 8A). Individual leaf traits previously shown to be associated with the leaf economics spectrum, such as presence/absence of teeth or lobes (Royer et al., 2012; Roth-Nebelsick et al., 2017), do not show meaningful differences in reconstructed LMA in our data set (Appendix S5). The fossil data set showing differentiated LMA for these two traits was geographically constrained to Europe (Roth-Nebelsick et al., 2017), while our data set is weighted toward North America, suggesting a need to control for phylogeny. Additionally, the error associated with LMA reconstruction (Royer et al., 2007) may mask correlations that otherwise manifest quite strongly in the modern record (Royer et al., 2012).

The only architectural traits with meaningful LMA differences at the species level are dentate vs. crenate teeth and acute vs. obtuse leaf base angles. Because the majority of dentate morphospecies (n=14) come from one depositional basin, additional samples are needed to confirm this result. Acute (n=138) and obtuse (n=85) base angle states are more comprehensively recorded, but why obtuse base angles are associated with faster return strategies is unclear. Obtuse bases suggest wider leaves, yet other width indicators (length:width ratio, lobation, palmate primary

venation) do not vary with LMA. Instead, this correlation may simply be a product of the petiole-width proxy: leaf mass concentrated toward the base of the leaf should require less structural support than leaf mass found toward the apex, potentially allowing a narrower petiole for the same total leaf mass.

Overall, our results provide little evidence that leaf architectural characters have a strong functional relation to the leaf economics spectrum or a significant impact on LMA. As few individual traits are convincingly correlated with LMA, we attribute the small correlation between leaf architecture and site-level LMA seen in our TCT analysis (Figure 8B) to the intertwined relationship of LMA with climate and phylogeny, which are both themselves strongly associated with aspects of leaf architecture (Little et al., 2010; Royer et al., 2012).

A final factor threatens every interpretation of fossil LMA: depositional environment, which plays a key role in taphonomic processes, can affect which species get preserved (Ellis and Johnson, 2013), and may filter for certain morphological characteristics (Spicer, 1981; Hagen et al., 2019). A significant depositional bias could have a determinative effect on which LMA cluster an assemblage of fossil leaves is sorted into, obscuring meaningful correlations and refracting our understanding of the viable leaf economic strategies at a site. Our results provide reason for optimism. While we find that species from lacustrine environments tend to have higher reconstructed species-mean LMA than species from fluvial environments, this species-level bias does not appear to be determinative at the site level. The three clusters commonly found in the fossil record are well represented among both lacustrine and fluvial sites (Figure 9). Like every other factor that we investigated, depositional environment does not, by itself, define site-mean LMA or LMA distribution, nor does it eliminate any particular leaf economic strategy from the fossil record.

Most of the discussion thus far has been concerned with the use of LMA in relation to leaf economics and plant strategy. However, LMA has some properties that are incidental to the leaf economic spectrum, which can be extremely useful in paleoecological interpretations. Sun leaves growing in the canopy tend to have higher LMA than shade leaves from the same tree, meaning that variance in reconstructed LMA could suggest the canopy position of a species (Cheesman et al., 2020). LMA is also frequently used in the study of fossil plant-insect interactions as a measure of herbivory resistance (Royer et al., 2007; Currano et al., 2008). Our results provide further support for these applications, particularly by minimizing the specter of depositional bias in reconstructions of LMA distributions.

## CONCLUSIONS

Species-mean leaf mass per area is, at its foundation, a reflection of leaf economics. The correlations that make up the leaf economics spectrum are stronger than the correlations between LMA and climate, phylogeny, morphospace,

or depositional environment, usually by an order of magnitude or more. Through our compilation and analysis of a fossil and modern LMA data set, we investigated whether site-level LMA distributions can be confidently attributed to climate, biome, or deciduousness, as has been done in paleobotanical research. Our results show that individual climatic variables, particularly those related to temperature seasonality, water availability, and irradiance, affect LMA distributions. However, we also find that despite these broad correlations, there is little to distinguish between individual sites. Shifts in climate may drive shifts in LMA distribution, but shifts in LMA distribution do not necessarily indicate a shift in climate or, importantly, biome. In fact, our results show that taxonomic composition and frequency of deciduous species at a site have similarly significant correlations with LMA distribution, leaving it difficult to attribute differences between LMA distributions to any one of these factors without additional context derived from non-LMA sources.

Reconstructions of fossil LMA must be considered the end point of the chain of causality, the leaf economic culmination of the influences of these many abiotic and biotic factors. Interpretations of fossil LMA should thus move back toward a focus on the fundamentals: the leaf economic strategies of individual morphospecies and the assembly of those strategies to form a site, all contextualized within taxonomic composition, depositional environment, and climate.

## **AUTHOR CONTRIBUTIONS**

M.J.B. and E.D.C. conceived and designed the research and acquired the data. E.D.C., M.J.B., and A.J.L. analyzed the data and drafted and revised the manuscript.

#### **ACKNOWLEDGMENTS**

The authors thank C. K. West and an anonymous reviewer for their thoughtful comments; T. Wappler, D. Royer, and D. Peppe for providing LMA data; and C. Strömberg for helpful discussions. Support was provided to E.D.C. by the National Science Foundation (ICER 2026961).

#### DATA AVAILABILITY STATEMENT

Data and materials to reproduce analyses can be found on GitHub at https://github.com/mjbutrim/fossilmodernLMA.

## ORCID

Matthew J. Butrim http://orcid.org/0000-0002-7869-380X Alexander J. Lowe http://orcid.org/0000-0002-2514-1008 Ellen D. Currano http://orcid.org/0000-0002-5242-8573

#### REFERENCES

Adler, P. B., R. Salguero-Gómez, A. Compagnoni, J. S. Hsu, J. Ray-Mukherjee, C. Mbeau-Ache, and M. Franco. 2014. Functional traits explain variation in plant life history strategies. *Proceedings of the National Academy of Sciences* 111: 740–745.

Allen, S. E., A. J. Lowe, D. J. Peppe, and H. W. Meyer. 2020. Paleoclimate and paleoecology of the latest Eocene Florissant flora of central Colorado, U.S.A. *Palaeogeography, Palaeoclimatology, Palaeoecology* 551: 109678.

- Anderegg, L. D. L. 2023. Why can't we predict traits from the environment? New Phytologist 237: 1998–2004.
- Bagaria, G., V. Granda, and G. Kunstler. 2022. ggbiome: Obtain and Plot Whittaker's Biome. R package version 0.0.1. Website: https://github.com/guillembagaria/ggbiome/
- Baraloto, C., C. E. Timothy Paine, L. Poorter, J. Beauchene, D. Bonal, A. Domenach, B. Hérault, et al. 2010. Decoupled leaf and stem economics in rain forest trees. *Ecology Letters* 13: 1338–1347.
- Barnosky, A. D., E. A. Hadly, P. Gonzalez, J. Head, P. D. Polly, A. M. Lawing, J. T. Eronen, et al. 2017. Merging paleobiology with conservation biology to guide the future of terrestrial ecosystems. *Science* 355: eaah4787.
- Bartlett, M. K., C. Scoffoni, R. Ardy, Y. Zhang, S. Sun, K. Cao, and L. Sack. 2012. Rapid determination of comparative drought tolerance traits: using an osmometer to predict turgor loss point. *Methods in Ecology and Evolution* 3: 880–888.
- Baumgartner, A., and D. J. Peppe. 2021. Paleoenvironmental changes in the Hiwegi Formation (lower Miocene) of Rusinga Island, Lake Victoria, Kenya. Palaeogeography, Palaeoclimatology, Palaeoecology 574: 110458.
- Blonder, B., D. L. Royer, K. R. Johnson, I. Miller, and B. J. Enquist. 2014. Plant ecological strategies shift across the Cretaceous–Paleogene boundary. PLoS Biology 12: 1–7.
- Bruelheide, H., J. Dengler, O. Purschke, J. Lenoir, B. Jiménez-Alfaro, S. M. Hennekens, Z. Botta-Dukát, et al. 2018. Global trait–environment relationships of plant communities. *Nature Ecology & Evolution* 2: 1906–1917.
- Brun, P., N. E. Zimmermann, C. Hari, L. Pellissier, and D. N. Karger. 2022. Global climate-related predictors at kilometer resolution for the past and future. *Earth System Science Data* 14: 5573–5603.
- Butrim, M. J., and D. L. Royer. 2020. Leaf-economic strategies across the Eocene-Oligocene transition correlate with dry season precipitation and paleoelevation. *American Journal of Botany* 107: 1772–1785.
- Butrim, M. J., D. L. Royer, I. M. Miller, M. Dechesne, N. Neu-Yagle, T. R. Lyson, K. R. Johnson, and R. S. Barclay. 2022. No Consistent Shift in Leaf Dry Mass per Area Across the Cretaceous—Paleogene Boundary. Frontiers in Plant Science 13: 894690.
- Carvalho, M. R., C. Jaramillo, F. de la Parra, D. Caballero-Rodríguez, F. Herrera, S. Wing, B. L. Turner, et al. 2021. Extinction at the end-Cretaceous and the origin of modern Neotropical rainforests. *Science* 372: 63–68.
- Cavender-Bares, J., A. Keen, and B. Miles. 2006. Phylogenetic structure of Floridian plant communities depends on taxonomic and spatial scale. *Ecology* 87: S109–S122.
- Chase, J. M., N. J. B. Kraft, K. G. Smith, M. Vellend, and B. D. Inouye. 2011. Using null models to disentangle variation in community dissimilarity from variation in  $\alpha$ -diversity. *Ecosphere* 2: 1–11.
- Cheesman, A. W., H. Duff, K. Hill, L. A. Cernusak, and F. A. McInerney. 2020. Isotopic and morphologic proxies for reconstructing light environment and leaf function of fossil leaves: A modern calibration in the Daintree Rainforest, Australia. American Journal of Botany 107: 1165–1176.
- Coble, A. P., and M. A. Cavaleri. 2015. Light acclimation optimizes leaf functional traits despite height-related constraints in a canopy shading experiment. *Oecologia* 177: 1131–1143.
- Cornwell, W. K., and D. D. Ackerly. 2009. Community assembly and shifts in plant trait distributions across an environmental gradient in coastal California. *Ecological Monographs* 79: 109–126.
- Currano, E. D., P. Wilf, S. L. Wing, C. C. Labandeira, E. C. Lovelock, and D. L. Royer. 2008. Sharply increased insect herbivory during the Paleocene–Eocene Thermal Maximum. *Proceedings of the National Academy of Sciences* 105: 1960–1964.
- Díaz, S., J. Kattge, J. H. C. Cornelissen, I. J. Wright, S. Lavorel, S. Dray, B. Reu, et al. 2016. The global spectrum of plant form and function. *Nature* 529: 167–171.
- Drost, H. 2018. Philentropy: Information Theory and Distance Quantification with R. *Journal of Open Source Software* 3: 765.

- Ellis, B., D. C. Daly, L. J. Hickey, K. R. Johnson, J. D. Mitchell, P. Wilf, and S. L. Wing. 2009. Manual of Leaf Architecture. New York Botanical Garden
- Ellis, B., and K. R. Johnson. 2013. Comparison of leaf samples from mapped tropical and temperate forests: Implications for interpretations of the diversity of fossil assemblages. *Palaios* 28: 163-177
- Eronen, J. T., P. D. Polly, M. Fred, J. Damuth, D. C. Frank, V. Mosbrugger,C. Scheidegger, et al. 2010. Ecometrics: the traits that bind the past and present together. *Integrative Zoology* 5: 88–101.
- Ferreira, L., and D. B. Hitchcock. 2009. A comparison of hierarchical methods for clustering functional data. Communications in Statistics-Simulation and Computation 38: 1925–1949.
- Fick, S. E., and R. J. Hijmans. 2017. WorldClim 2: new 1-km spatial resolution climate surfaces for global land areas. *International Journal of Climatology* 37: 4302–4315.
- Flores, O., E. Garnier, I. J. Wright, P. B. Reich, S. Pierce, S. Diaz, R. J. Pakeman, et al. 2014. An evolutionary perspective on leaf economics: phylogenetics of leaf mass per area in vascular plants. *Ecology* and Evolution 4: 2799–2811.
- Flynn, A. G., and D. J. Peppe. 2019. Early Paleocene tropical forest from the Ojo Alamo Sandstone, San Juan Basin, New Mexico, USA. *Paleobiology* 45: 612–635.
- Foster, G. L., D. L. Royer, and D. J. Lunt. 2017. Future climate forcing potentially without precedent in the last 420 million years. *Nature Communications* 8: 14845.
- Fyllas, N. M., S. Patiño, T. R. Baker, G. Bielefeld Nardoto, L. A. Martinelli, C. A. Quesada, R. Paiva, et al. 2009. Basin-wide variations in foliar properties of Amazonian forest: phylogeny, soils and climate. *Biogeosciences* 6: 2677–2708.
- Gomarasca, U., M. Migliavacca, J. Kattge, J. A. Nelson, Ü. Niinemets, C. Wirth, A. Cescatti, et al. 2023. Leaf-level coordination principles propagate to the ecosystem scale. *Nature Communications* 14: 3948.
- Gonzalez-Akre, E., W. McShea, N. Bourg, and K. Anderson-Teixeira. 2015. Leaf traits data (SLA) for 56 woody species at the Smithsonian Conservation Biology Institute-ForestGEO Forest Dynamic Plot. Front Royal, Virginia. USA. [Data set]. Version 1.0. Website: https://try-db.org/
- Gower, J. C. 1971. A general coefficient of similarity and some of its properties. *Biometrics* 27: 857–871.
- Gutiérrez, E., D. Gutiérrez, R. Morcuende, A. L. Verdejo, S. Kostadinova, R. Martinez-Carrasco, and P. Pérez. 2009. Changes in leaf morphology and composition with future increases in CO2 and temperature revisited: Wheat in field chambers. *Journal of Plant Growth Regulation* 28: 349–357.
- Gutschick, V. P., and F. W. Wiegel. 1988. Optimizing the canopy photosynthetic rate by patterns of investment in specific leaf mass. *The American Naturalist* 132: 67–86.
- Haber, L. T., R. T. Fahey, S. B. Wales, N. Correa Pascuas, W. S. Currie, B. S. Hardiman, and C. M. Gough. 2020. Forest structure, diversity, and primary production in relation to disturbance severity. *Ecology* and Evolution 10: 4419–4430.
- Hagen, E. R., D. L. Royer, R. A. Moye, and K. R. Johnson. 2019. No large bias within species between the reconstructed areas of complete and fragmented fossil leaves. *Palaios* 34: 43–48.
- Hanley, M. E., B. B. Lamont, M. M. Fairbanks, and C. M. Rafferty. 2007.Plant structural traits and their role in anti-herbivore defence.Perspectives in Plant Ecology, Evolution and Systematics 8: 157–178.
- Herben, T., J. Klimešová, and M. Chytrý. 2018. Effects of disturbance frequency and severity on plant traits: an assessment across a temperate flora. Functional Ecology 32: 799–808.
- Hickey, L. J. 1977. Stratigraphy and paleobotany of the Golden Valley Formation (early Tertiary) of western North Dakota. GSA Memoirs 150. https://doi.org/10.1130/MEM150
- Hothorn, T., F. Bretz, and P. Westfall. 2008. Simultaneous Inference in General Parametric Models. *Biometrical Journal* 50: 346–363.

- Johnson, K. R. 2002. Megaflora of the Hell Creek and lower Fort Union Formations in the western Dakotas: Vegetational response to climate change, the Cretaceous-Tertiary boundary event, and rapid marine transgression. Special Paper of the Geological Society of America 361: 329–391.
- Kattge, J., G. Bönisch, S. Díaz, S. Lavorel, I. C. Prentice, P. Leadley, S. Tautenhahn, et al. 2020. TRY plant trait database–enhanced coverage and open access. Global Change Biology 26: 119–188.
- Kearsley, E., H. Verbeeck, K. Hufkens, F. Van de Perre, S. Doetterl, G. Baert, H. Beeckman, et al. 2017. Functional community structure of African monodominant Gilbertiodendron dewevrei forest influenced by local environmental filtering. *Ecology and Evolution* 7: 295–304.
- Kindt, R. 2020. WorldFlora: An R package for exact and fuzzy matching of plant names against the World Flora Online taxonomic backbone data. *Applications in Plant Sciences* 8: e11388.
- Kraft, N. J. B., and D. D. Ackerly. 2010. Functional trait and phylogenetic tests of community assembly across spatial scales in an Amazonian forest. *Ecological monographs* 80: 401–422.
- Laliberté, E., P. Legendre, and B. Shipley. 2014. FD: measuring functional diversity from multiple traits, and other tools for functional ecology. R package version 1.0-12.3.
- Lamanna, C., B. Blonder, C. Violle, N. J. B. Kraft, B. Sandel, I. Šímová, J. C. Donoghue, et al. 2014. Functional trait space and the latitudinal diversity gradient. Proceedings of the National Academy of Sciences of the United States of America 111: 13745–13750.
- Lin, J. 1991. Divergence measures based on the Shannon entropy. IEEE Transactions on Information Theory 37: 145–151.
- Little, S. A., S. W. Kembel, and P. Wilf. 2010. Paleotemperature proxies from leaf fossils reinterpreted in light of evolutionary history. PLoS One 5: e15161.
- Lowe, A. J., D. R. Greenwood, C. K. West, J. M. Galloway, M. Sudermann, and T. Reichgelt. 2018. Plant community ecology and climate on an upland volcanic landscape during the Early Eocene Climatic Optimum: McAbee Fossil Beds, British Columbia, Canada. *Palaeogeography*, *Palaeoclimatology*, *Palaeoecology* 511: 433–448.
- Lyson, T. R., I. M. Miller, A. D. Bercovici, K. Weissenburger, A. J. Fuentes, W. C. Clyde, J. W. Hagadorn, et al. 2019. Exceptional continental record of biotic recovery after the Cretaceous-Paleogene mass extinction. *Science* 366: 977–983.
- Mason, N. W. H., F. De Bello, J. Doležal, and J. Lepš. 2011. Niche overlap reveals the effects of competition, disturbance and contrasting assembly processes in experimental grassland communities. *Journal* of *Ecology* 99: 788–796.
- McCune, B., and J. B. Grace. 2002. Analysis of ecological communities. MjM Software Design, Oregon, USA.
- Messier, J., B. J. McGill, and M. J. Lechowicz. 2010. How do traits vary across ecological scales? A case for trait-based ecology. *Ecology Letters* 13: 838–848.
- Messier, J., B. J. McGill, B. J. Enquist, and M. J. Lechowicz. 2017. Trait variation and integration across scales: is the leaf economic spectrum present at local scales? *Ecography* 40: 685–697.
- Moles, A. T., S. E. Perkins, S. W. Laffan, H. Flores-Moreno, M. Awasthy, M. L. Tindall, L. Sack, et al. 2014. Which is a better predictor of plant traits: temperature or precipitation? *Journal of Vegetation Science* 25: 1167–1180.
- Niinemets, Ü. 2001. Global-scale climatic controls of leaf dry mass per area, density, and thickness in trees and shrubs. *Ecology* 82: 453–469.
- Norby, R. J., J. D. Sholtis, C. A. Gunderson, and S. S. Jawdy. 2003. Leaf dynamics of a deciduous forest canopy: no response to elevated CO2. *Oecologia* 136: 574–584.
- Oksanen, J., G. L. Simpson, F. G. Blanchet, R. Kindt, P. Legendre, P. R. Minchin, R. B. O'Hara, et al. 2022. vegan: Community Ecology Package, R package version 2.6-4. Website: https://CRAN.R-project.org/package=vegan/
- Ordoñez, J. C., P. M. Van Bodegom, J. M. Witte, I. J. Wright, P. B. Reich, and R. Aerts. 2009. A global study of relationships between leaf traits,

- climate and soil measures of nutrient fertility. *Global Ecology and Biogeography* 18: 137–149.
- Paine, C. E. T., C. Baraloto, J. Chave, and B. Hérault. 2011. Functional traits of individual trees reveal ecological constraints on community assembly in tropical rain forests. Oikos 120: 720–727.
- Penuelas, J., J. Sardans, J. Llusia, S. M. Owen, J. Carnicer, T. W. Giambelluca, E. L. Rezende, et al. 2010. Faster returns on 'leaf economics' and different biogeochemical niche in invasive compared with native plant species. Global Change Biology 16: 2171–2185.
- Peppe, D. J., D. L. Royer, P. Wilf, and E. A. Kowalski. 2010. Quantification of large uncertainties in fossil leaf paleoaltimetry. *Tectonics* 29(TC3015): 1–14. https://doi.org/10.1029/2009TC002549
- Peppe, D. J., D. L. Royer, B. Cariglino, S. Y. Oliver, S. Newman, E. Leight, G. Enikolopov, et al. 2011. Sensitivity of leaf size and shape to climate: Global patterns and paleoclimatic applications. *New Phytologist* 190: 724–739.
- Peppe, D., A. Baumgartner, A. Flynn, and B. Blonder. 2018. Reconstructing Paleoclimate and Paleoecology Using Fossil Leaves. Methods in Paleoecology: Reconstructing Cenozoic Terrestrial Environments and Ecological Communities, 289–317. Springer International Publishing AG.
- Peterson, A. G., J. T. Ball, Y. Luo, C. B. Field, P. S. Curtis, K. L. Griffin, C. A. Gunderson, et al. 1999. Quantifying the response of photosynthesis to changes in leaf nitrogen content and leaf mass per area in plants grown under atmospheric CO2 enrichment. *Plant, Cell & Environment* 22: 1109–1119.
- Pinho, B. X., M. Tabarelli, C. J. F. terBraak, S. J. Wright, V. Arroyo-Rodríguez, M. Benchimol, B. M. J. Engelbrecht, et al. 2021. Functional biogeography of Neotropical moist forests: Trait-climate relationships and assembly patterns of tree communities. Global Ecology and Biogeography 30: 1430–1446.
- Podani, J. 1999. Extending Gower's general coefficient of similarity to ordinal characters. *Taxon* 48: 331–340.
- Poorter, L., and F. Bongers. 2006. Leaf traits are good predictors of plant performance across 53 rain forest species. *Ecology* 87: 1733–1743.
- Poorter, H., Ü. Niinemets, L. Poorter, I. J. Wright, and R. Villar. 2009. Causes and consequences of variation in leaf mass per area (LMA): A meta-analysis. New Phytologist 182: 565–588.
- R Core Team. 2023. R: A Language and Environment for Statistical Computing. R Foundation for Statistical Computing, Vienna, Austria. Website: https://www.R-project.org/
- Reich, P. B. 2014. The world-wide 'fast-slow'plant economics spectrum: a traits manifesto. *Journal of Ecology* 102: 275–301.
- Reich, P. B., M. B. Walters, and D. S. Ellsworth. 1991. Leaf age and season influence the relationships between leaf nitrogen, leaf mass per area and photosynthesis in maple and oak trees. *Plant, Cell & Environment* 14: 251–259.
- Roth-Nebelsick, A., M. Grein, C. Traiser, K. Moraweck, L. Kunzmann, J. Kovar-Eder, J. Kvaček, et al. 2017. Functional leaf traits and leaf economics in the Paleogene A case study for Central Europe. *Palaeogeography, Palaeoclimatology, Palaeoecology* 472: 1–14.
- Royer, D. L., R. A. Berner, and D. J. Beerling. 2001. Phanerozoic atmospheric CO2 change: evaluating geochemical and paleobiological approaches. *Earth-Science Reviews* 54: 349–392.
- Royer, D. L., L. Sack, P. Wilf, C. H. Lusk, G. J. Jordan, Ü. Niinemets, I. J. Wright, et al. 2007. Fossil leaf economics quantified: calibration, Eocene case study, and implications. *Paleobiology* 33: 574–589.
- Royer, D. L., I. M. Miller, D. J. Peppe, and L. J. Hickey. 2010. Leaf economic traits from fossils support a weedy habit for early angiosperms. American Journal of Botany 97: 438–445.
- Royer, D. L., D. J. Peppe, E. A. Wheeler, and Ü. Niinemets. 2012. Roles of climate and functional traits in controlling toothed vs. untoothed leaf margins. *American Journal of Botany* 99: 915–922.
- Simpson, A. H., S. J. Richardson, and D. C. Laughlin. 2016. Soil-climate interactions explain variation in foliar, stem, root and reproductive traits across temperate forests. Global Ecology and Biogeography 25: 964–978.

- Sokal, R., and F. Rohlf. 2012. Biometry. 4th ed. WH Freeman and Company, New York, USA.
- Spicer, R. A. 1981. The Sorting and Deposition of Allochthonous Plant Material in a Modern Environment at Silwood Lake, Silwood Park, Berkshire, England. U.S. Geological Survey Professional Papers 1143: 1–73.
- Stiles, E., P. Wilf, A. Iglesias, M. A. Gandolfo, and N. R. Cuneo. 2020. Cretaceous-Paleogene plant extinction and recovery in Patagonia. *Paleobiology* 46: 445–469.
- Swaine, E. K. 2007. Ecological and evolutionary drivers of plant community assembly in a Bornean rain forest. Ph.D. dissertation, University of Aberdeen, Aberdeen, Scotland.
- Swenson, N. G., B. J. Enquist, J. Pither, A. J. Kerkhoff, B. Boyle, M. D. Weiser, J. J. Elser, et al. 2012. The biogeography and filtering of woody plant functional diversity in North and South America. Global Ecology and Biogeography 21: 798–808.
- Vermillion, W. A., P. D. Polly, J. J. Head, J. T. Eronen, and A. M. Lawing. 2018. Ecometrics: a trait-based approach to paleoclimate and paleoenvironmental reconstruction: Reconstructing Cenozoic terrestrial environments and ecological communities. *In*: Methods in paleoecology, 373–394. Springer.
- Wagner, J. D., D. J. Peppe, J. M. K. O'keefe, and C. N. Denison. 2023. Plant Community Change across the Paleocene-Eocene Boundary in the Gulf Coastal Plain, Central Texas. *Palaios* 38: 436–451.
- Wang, H., S. P. Harrison, I. C. Prentice, Y. Yang, F. Bai, H. F. Togashi, M. Wang, et al. 2018. The China plant trait database: Toward a comprehensive regional compilation of functional traits for land plants. *Ecology* 99: 500.
- West, C. K., D. R. Greenwood, T. Reichgelt, A. J. Lowe, J. M. Vachon, and J. F. Basinger. 2020. Paleobotanical proxies for early Eocene climates and ecosystems in northern North America from middle to high latitudes. *Climate of the Past* 16: 1387–1410.
- West, C. K., T. Reichgelt, and J. F. Basinger. 2021. The Ravenscrag Butte flora: Paleoclimate and paleoecology of an early Paleocene (Danian) warm-temperate deciduous forest near the vanishing inland Cannonball Seaway. Palaeogeography, Palaeoclimatology, Palaeoecology 576: 110488.
- Wieczynski, D. J., B. Boyle, V. Buzzard, S. M. Duran, A. N. Henderson, C. M. Hulshof, A. J. Kerkhoff, et al. 2019. Climate shapes and shifts functional biodiversity in forests worldwide. *Proceedings of the National Academy of Sciences* 116: 587–592.
- Wieczynski, D. J., P. Singla, A. Doan, A. Singleton, Z.-Y. Han, S. Votzke, A. Yammine, and J. P. Gibert. 2021. Linking species traits and demography to explain complex temperature responses across levels of organization. Proceedings of the National Academy of Sciences 118: e2104863118.
- Wilf, P. 1997. When are leaves good thermometers? a new case for leaf margin analysis. *Paleobiology* 23: 373–390.
- World Flora Online (WFO). 2024. Website: http://www.worldfloraonline.org/
  Wright, I. J., M. Westoby, and P. B. Reich. 2002. Convergence towards higher leaf mass per area in dry and nutrient-poor habitats has different consequences for leaf life span. *Journal of Ecology* 90: 534–543.
- Wright, I. J., P. B. Reich, M. Westoby, D. D. Ackerly, Z. Baruch, F. Bongers, J. Cavender-Bares, et al. 2004. The worldwide leaf economics spectrum. *Nature* 428: 821–827.
- Wright, I. J., P. B. Reich, J. H. C. Cornelissen, D. S. Falster, P. K. Groom, K. Hikosaka, W. Lee, et al. 2005. Modulation of leaf economic traits and trait relationships by climate. *Global Ecology and Biogeography* 14: 411–421.
- Wright, I. J., D. D. Ackerly, F. Bongers, K. E. Harms, G. Ibarra-Manriquez, M. Martinez-Ramos, S. J. Mazer, et al. 2007. Relationships among ecologically important dimensions of plant trait variation in seven Neotropical forests. *Annals of Botany* 99: 1003–1015.
- Yang, J., R. A. Spicer, T. E. V Spicer, N. C. Arens, F. M. B. Jacques, T. Su, E. M. Kennedy, et al. 2015. Leaf form-climate relationships on the global stage: an ensemble of characters. Global Ecology and Biogeography 24: 1113–1125.

#### SUPPORTING INFORMATION

Additional supporting information can be found online in the Supporting Information section at the end of this article.

### Appendix S1.

- **Table S1.** Leaf architectural character states assigned to fossil leaves.
- **Table S2.** TRY data sets used in the modern leaf mass per area data set.
- **Table S3.** Morphospecies-mean leaf mass per area data for fossil data set.
- **Table S4.** Site-level information for fossil sites.
- **Table S5.** Species-mean leaf mass per area data for modern data set.
- **Table S6.** Site-level information for modern sites.
- Table S7. Linear regression model outputs.
- **Table S8.** Covariance between gridded climate variables.
- **Appendix S2.** Whittaker biome assignments for each locality with available mean annual temperature and mean annual precipitation measurements or reconstructions.
- Appendix S3. Linear and quadratic regressions between site mean leaf mass per area (LMA) and (A) mean annual temperature; (B) mean annual precipitation; (C) surface downwelling shortwave radiation (RSDS); (D) temperature seasonality; and (E) vapor pressure deficit.
- **Appendix S4.** Box and whisker plots showing how site-level distribution measures are associated with the leaf mass per area (LMA) distribution clusters.
- **Appendix S5.** Principal component analysis ordination illustrating how leaf mass per area (LMA) distribution clusters are spread across multivariate climate space.
- **Appendix S6.** Box and whisker plots showing how morphospecies leaf mass per area (LMA) is distributed across the character states of 11 leaf architectural characters.
- **Appendix S7.** Box and whisker plots of morphospecies leaf mass per area (LMA) for each analyzed trait combination type.

How to cite this article: Butrim, M. J., A. J. Lowe, and E. D. Currano. 2024. Leaf mass per area: An investigation into the application of the ubiquitous functional trait from a paleobotanical perspective. *American Journal of Botany* 111(10): e16419. https://doi.org/10.1002/ajb2.16419